Basalt-seawater interaction at near-supercritical conditions (400˚C, 500 bar): Hydrothermal alteration in the sub-seafloor

Mauro Passarella[a,b,*], Bruce W. Mountain[a], Terry M. Seward[b]

[a*]*GNS Science, Department of Geothermal Sciences, Wairakei, New Zealand*

[b]*School of Geography, Environment and Earth Sciences, Victoria University of Wellington, New Zealand*

* m.passarella@gns.cri.nz

Keywords: *Experimental geochemistry, near-supercritical, hydrothermal, seawater, sulfate mineral precipitation; elemental flux, trace elements*

ABSTRACT

Experiments are currently underway to simulate basalt-seawater interaction using a continuous flow reactor at near-supercritical conditions for seawater (400˚C, 500 bar). These conditions are typical of the supercritical reaction zone of mid-ocean ridge hydrothermal systems. The experimental set-up consists of two pressure vessels in series: a preheater vessel with a high temperature gradient (40 – 377˚C) containing zirconia (ZrO_2) beads and a reactor vessel at 400˚C to contain the rock material. In the experiment reported here, seawater was pumped through the system while being heated to 400˚C, 500 bar without rock material in the reactor vessel. The seawater was first filtered to remove microflora and then deoxygenated. Continuous flow was maintained at 1 ml hr^{-1} during the experiment. Chemical analysis show a loss of Ca (from 360 to 75 mg kg^{-1}), Mg (from 1010 to 370 mg kg^{-1}) and SO_4 (from 2020 to 120 mg kg^{-1}) from the seawater. SEM analysis confirm the presence of anhydrite, Mg-sulfate minerals (epsomite and/or caminite) and brucite. Mineral saturation indices show that the reacted seawater is in equilibrium with brucite and anhydrite at 400ºC. The seawater is depleted in calcium, magnesium and sulfate due to the precipitation of retrograde solubility phases. This is consistent with the seawater having a very low pH (3.0). It is conjectured that this process occurs within hours. Further experiments are underway to react this modified seawater for basalt material.

1. INTRODUCTION

Mid-ocean ridges and seafloor spreading centers are regions of the earth’s crust where large volumes of rock are affected by supercritical fluid-rock interactions. Under supercritical conditions, physical-chemical properties of the fluid change from polar to non-polar in behaviour and fluid has a strong propensity to hydrate ions, substantially controlling metal transport.

There are few modern experimental studies aimed at understanding these hydrothermal reactions and their kinetics. Although several experimental studies have been carried out in the past, giving important insight into the fluid-rock exchanges, many fundamental questions involving the equilibrium and kinetic aspects of seawater-rock interaction still remain. The experimental approach offers an alternative to study the fluid-mineral interactions that occur in these environments especially when computer modeling is not possible due to a lack of reliable thermodynamic data.

Submarine hydrothermal systems develop where two oceanic plates diverge forming a central ridge. Fluid circulates on both sides of the ridge in essentially three main zones: a zone of “recharge”, a zone of “reaction” and a zone of “discharge or up-welling”. The zone of recharge is composed of volcanic sediments, basalt, pillow-lava and breccia while the zone of reaction is made of a sheeted dike complexes and gabbros.

During this circulation, there are changes in the mineral composition of the oceanic crust and of seawater chemistry regulated by fluid-rock interaction. Cold seawater descends at the recharge zone through fractures far from the ridge. This fluid becomes heated to subcritical and eventually supercritical conditions in the reaction zone (4-5 km depth). Here, uprising magma heats circulating fluid which rises buoyantly to the seafloor through an up-welling zone forming the hydrothermal vents we see at the mid-ocean ridges.

The chemistry at the vents provides an important record of the alteration, temperature and pressure conditions that the seawater experienced during passage within the crust. Geochemical analysis around plumes reveal that the steady state concentrations of dissolved species and their solubility are controlled by mineral phases occurring in the reaction zone. These are the deepest areas of a submarine hydrothermal system where the fluid circulation occurs just above the magmatic heating source, close to the brittle-ductile boundary. Here, the alteration process is at its maximum and the kinetics of chemical reactions are faster due to the high T and P conditions ($T \geq 400$˚C, 500 bar).

2. EXPERIMENTAL METHOD

The high P-T hydrothermal apparatus used (Fig. 1) allows simulation of fluid-rock interactions at temperatures and pressures up to 400˚C and 500 bar. Continuous flow is achieved by a computer-controlled double-piston pump with a flow rate range of 0.001 - 15 ml min^{-1} (Passarella et al., 2015; Passarella et al., 2016; Sonney and Mountain, 2013). For seawater experiments, two pressure vessels were used. The first, called the preheater (56 cm length x 2 cm dia), is half-filled with zirconia (ZrO_2) beads. The second, called the reactor (15 cm length x 2 cm dia), holds the rock material. Both pressure vessels and all wetted surfaces are constructed of titanium or hastelloy.

The preheater has a volume of 71 ml. Approximately 20 cm of the column extend outside the oven while the remainder extends down to the bottom of the oven. This creates a temperature gradient between the top (40˚C) and bottom (377˚C) of the column. An electric fan is used to keep the top of the column cool. The zirconia beads provide a large surface area for retrograde phases, such as anhydrite, to precipitate before the seawater exits the bottom of the column. This prevents scaling of the exit tubing while at the same time allowing actual seawater to enter the reactor vessel.

The first experiment used the preheater set-up as shown Figure 1 without basalt in the reactor. This experiment was designed to measure the background chemistry of the fluid after reaction with the zirconia but without influence from basalt. The second experiment will use the preheater packed with zirconia as shown in Figure 1 and the reactor will contain basalt fragments as well as an 8 x 8 mm block of basalt. Continuous flow is maintained at 1 ml·hr^{-1} for both experiments.

The basalt, sourced from Reykjanes, Iceland, is devoid of any secondary mineralisation or alteration. It is composed mainly of plagioclase (labradorite/bytownite) and clinopyroxene (augite), with lesser opaques (iron and titanium oxides), minor olivine and volcanic glass. The rock was crushed, sieved and cleaned to obtain the 355-500 µm size fraction. The zirconia beads are composed of predominantly ZrO_2 (97%) and MgO (3%) with minor concentration at > 0.30% of SiO_2, CaO, Fe_2O_3, Al_2O_3, TiO_2. The fluid used was seawater collected at the National Aquarium in Napier, New Zealand. It was first filtered to remove microflora and then deoxygenated.

All fluid samples were analysed for major cations (Li, Na, K, Mg, Ca, Sr, Mn, Fe, As, Al, B, and SiO_2) by ICP-OES, anions (Cl^- and SO_4^{2-}) by IC and H_2S by UV-Vis spectroscopy. Quench pH was measured by electrode at room temperature and then recalculated for 400˚C and 500 bar.

SEM-EDS analysis was done to characterise the mineralogy of the precipitates that formed in the preheater vessel.

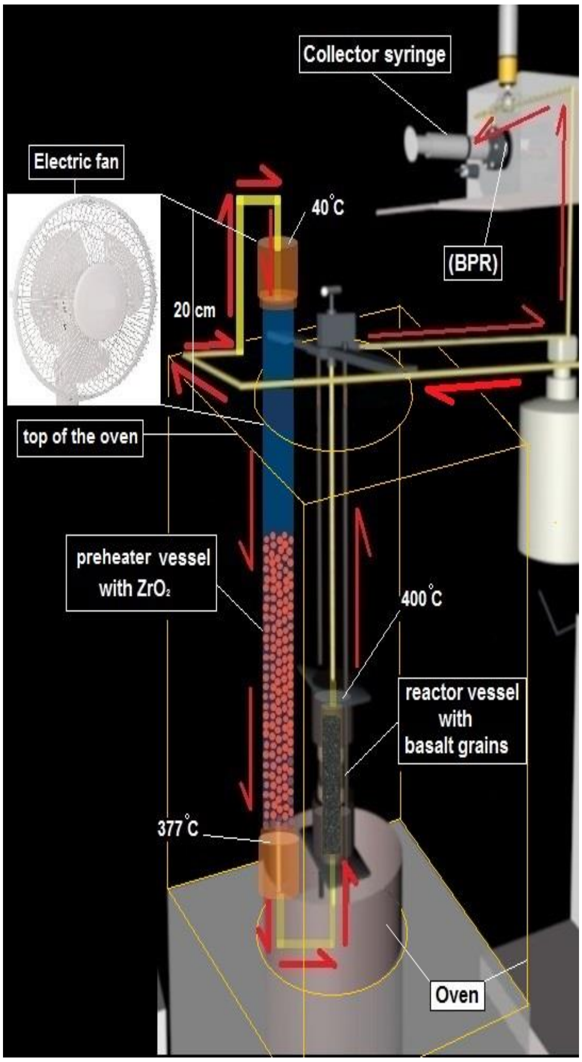

Figure 1. Experimental apparatus. Two pressure vessels are positioned in series in the oven. The preheater vessel contains ZrO_2 beads to allow sulfate mineral precipitation as the seawater descends. There is a temperature gradient from 40˚C at the top to 377˚C at the bottom of the vessel. The reactor vessel contains the rock material where the preheated seawater enters at 400˚C. The experimental solution is collected in a plastic syringe positioned after the back pressure regulator (BPR). Red arrows show the direction of flow of the solution.

3. RESULTS

3.1 Preliminary results of the basalt-seawater experiment

In the first experiment, seawater was used but no rock was present in the reactor vessel. This was undertaken to test for mineral precipitation in the preheater and to determine the background concentration from the zirconia beads. The experiment ran for a total of 31 days. Initially, distilled water was pumped through the system for the five days to measure mobility of elements from the zirconia at 400°C, 500 bar. After five days, the fluid was switched to seawater which passed through the apparatus at 400˚C, 500 bar for 26 days. Chloride concentrations (Fig. 2) show that it took about seven days (168 hours) for the seawater to completely displace the distilled water at 1 ml hr^{-1}.

The room temperature pH of the unreacted Napier seawater is 7.75 (Fig. 2). The Napier seawater is more dilute (15,700 mg kg^{-1} Cl) with respect to average seawater (19,400 mg kg^{-1} Cl) due to freshwater inflow from the Clive River to the south. Fe and SiO_2 in the starting seawater were <0.1 and <0.1 mg kg^{-1}, respectively.

During the initial five days of distilled water flow, effluent pH dropped from 6.8 to 5.5, due to reaction with the zirconia beads. After switching to seawater, the pH decreased over three days to a stable value of 3.0 for the remainder of the experiment.

During the first five days, measurable concentrations of SiO_2 were found. This originated from the zirconia. After switching to seawater, changes from starting composition included: a decrease in Ca from 360 to 75 mg kg^{-1}; Mg from 1010 to 370 mg kg^{-1}; SO_4 from 2020 to 120 mg kg^{-1}; Na from 9600 to 8500 mg kg^{-1}. Cl and K concentrations reached steady values similar to the starting seawater. Fe and SiO_2

increased to up to 85 mg kg^{-1} and 70 mg kg^{-1}, respectively. There was an increase in SiO_2 and a decrease in Fe during the last five days of the experiment.
Visual examination shows that unreacted beads are golden yellow in colour (Fig. 3a). Beads removed from the bottom of the preheater showed extensive deposits of white mineral material and had changed colour slightly (Fig. 3b).

SEM examination of the white mineral precipitates found on the zirconia beads shows coarsely crystalline material (Fig. 4a,b). EDS backscatter images at low magnification showed this material to be composed of mainly epsomite ($MgSO_4 \cdot 7H_2O$) or possibly caminite ($Mg_7(SO_4)_5(OH)_4 \cdot H_2O$) with lesser amounts of anhydrite ($CaSO_4$) (Fig. 4c-f).

Figure 5 shows close-up photographs of the surface of the zirconia beads. They have deposits with an overall polygonal shape. These deposits are composed of brucite ($Mg(OH)_2$).

The experiment using zirconia-seawater-basalt is presently underway.

4. DISCUSSION

The heating of seawater up to 400°C, 500 bar without interaction with rock material is necessary to: 1) precipitate mineral phases with retrograde solubility preventing blockage of the tubing and rock material; 2) determine the input composition from the preheater into the reactor. The gradient along the preheater is necessary to allow entry of seawater into its large volume where crystallisation will not cause blockage. As the water descends through the large preheater vessel, crystallisation of retrograde solubility minerals occurs. This simulates, to some degree, the natural process of fluid recharge occurring at mid-ocean ridge during its penetration within the oceanic crust. It reproduces the formation of Ca-Mg-sulphate minerals such as anhydrite, epsomite or possibly caminite and brucite (Seyfried *et al.*, 1988).

The mineral precipitation in the preheater vessel depleted the seawater of Ca, Mg, SO_4 and perhaps a small amount of Na. The precipitation of anhydrite and Mg-sulfate occurred in the bottom half of the preheater that contained the zirconia while brucite was found only at the bottom. It is unclear what mechanism causes the brucite to precipitate in the polygonal forms.

The speed of the precipitation reactions during seawater flow up to near-supercritical conditions shifted the pH to highly acid values of 3.0. This can be explained by the precipitation of sulfate minerals and brucite. Mg and Ca are present in seawater in high concentrations predominantly as Mg^{2+} and Ca^{2+} along with Mg and Ca chloride complexes. The precipitation of brucite (a) and caminite (b) (or MHSH(Mg1.5) (c), anhydrite (d), and epsomite (e), reduce pH. The mechanism can be explained by the following reactions:

$$Mg^{2+} + 2H_2O \leftrightarrow Mg(OH)_2 + 2H^+ \tag{a}$$
$$7Mg^{2+} + 5SO_4^{2-} + 5H_2O \leftrightarrow Mg_7(SO_4)_5(OH)_4 \cdot H_2O + 4H^+ \tag{b}$$
$$1.5\,Mg^{2+} + SO_4^{2-} + H_2O \leftrightarrow MHSH(Mg1.5) + H^+ \tag{c}$$
$$Ca^{2+} + HSO_4^{-} \leftrightarrow CaSO_4 + H^+ \tag{d}$$
$$Mg^{2+} + HSO_4^{-} + 7H_2O \leftrightarrow MgSO_4 \cdot 7H_2O + H^+ \tag{e}$$

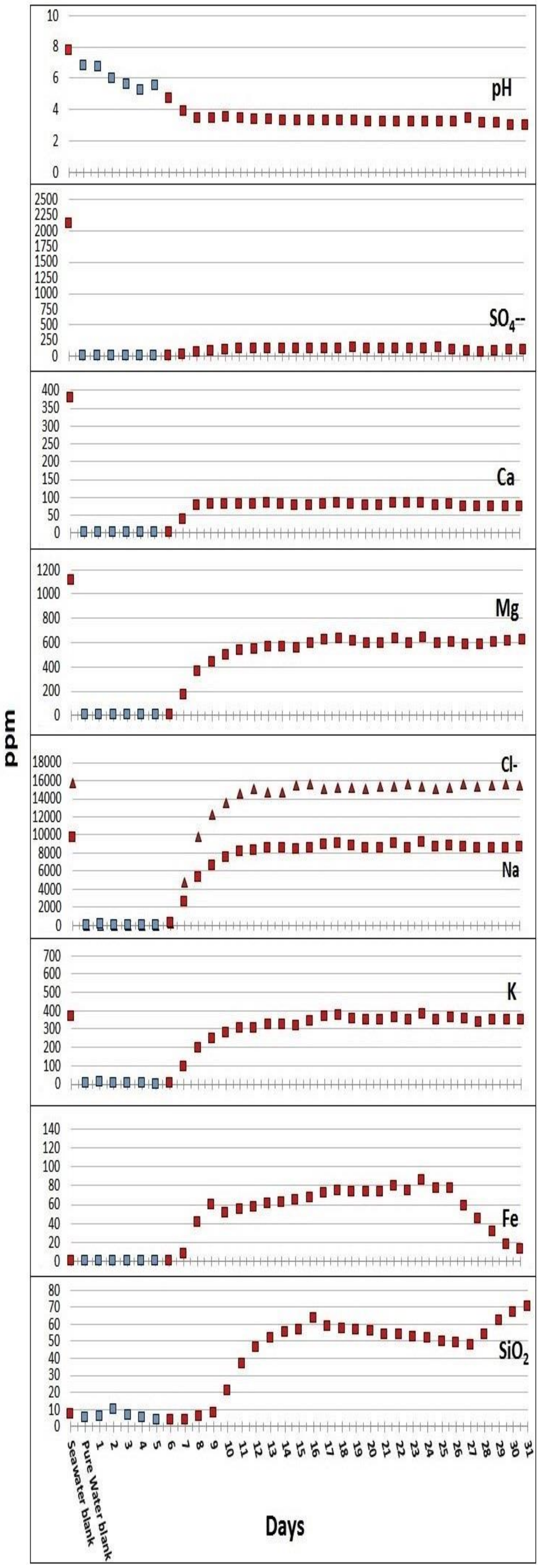

Figure 2. Starting composition of unreacted seawater and distilled water and effluent composition versus time.

Figure 3. Photographs of a) unreacted zirconia (ZrO_2) beads, ~2 mm dia; b) zirconia beads collected at the bottom of the preheater after the experiment. Note the extensive precipitation of secondary mineral material.

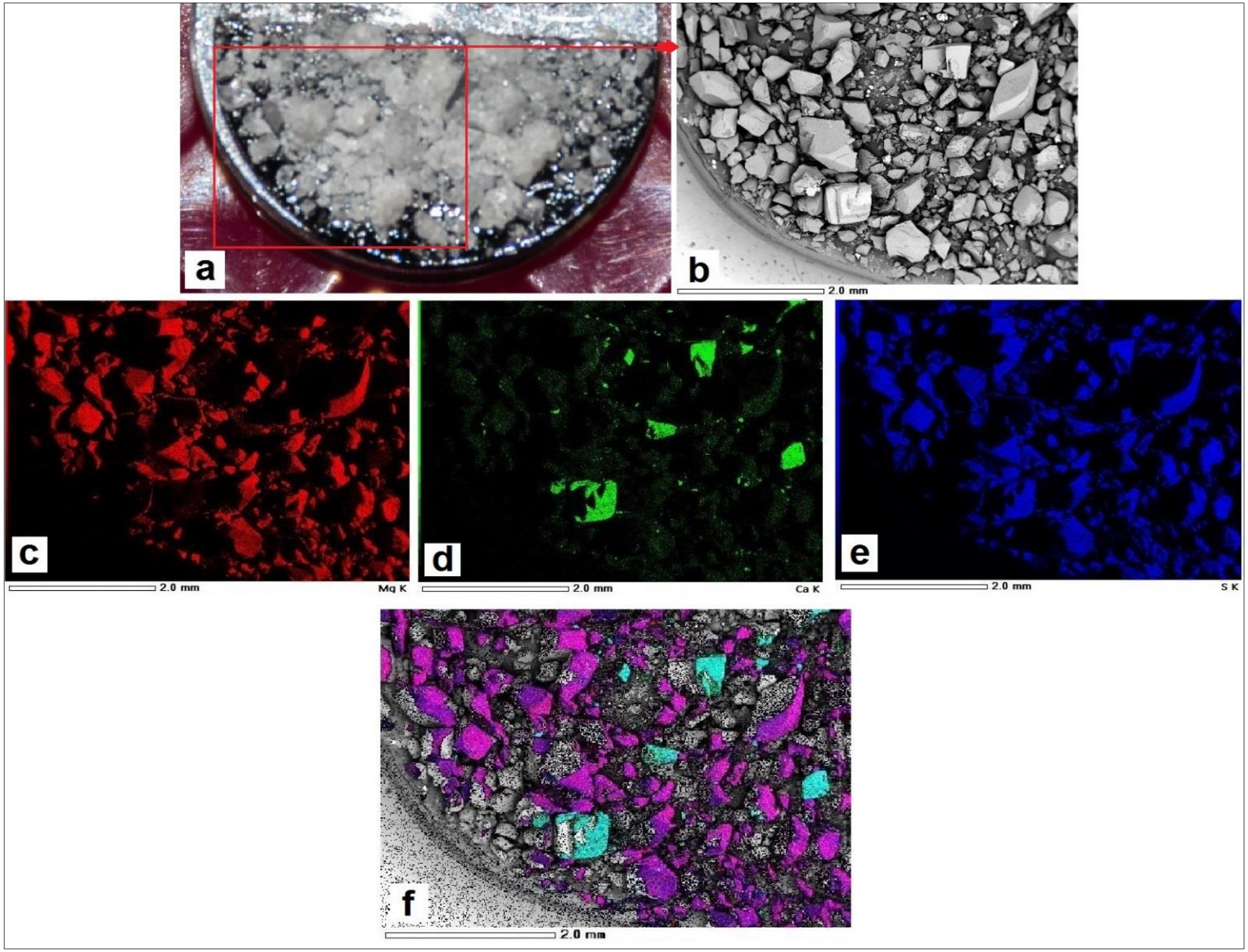

Figure 4. SEM photographs of mineral precipitates from the zirconia only experiment. a) digital photograph of white precipitate removed from beads; b) SEM photograph of a portion of the area in a); c) -d)-e) elemental maps of the sample in b) for Mg, Ca, and S; f) composite elemental map showing distinct grains of Mg sulfate (violet) and anhydrite (light blue).

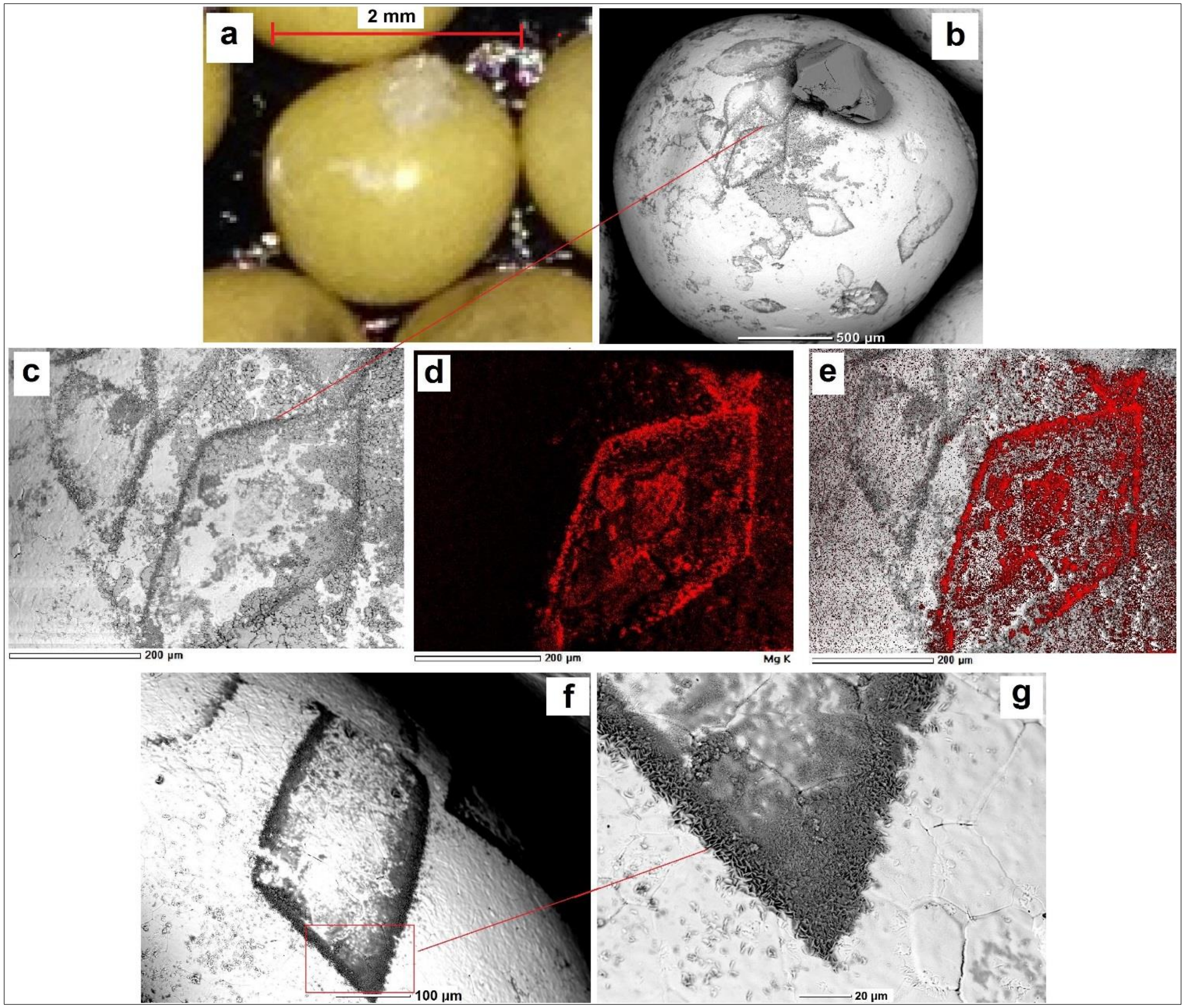

Figure 5. SEM photographs of the surface of the zirconia beads. a) Digital showing a bead with a Mg sulfate crystal; b)-c) SEM photographs of a) showing the polygonal growths of brucite; d) – e) elemental maps showing Mg concentration of polygonal deposit in c); f) – g) SEM photographs of a second zirconia bead showing a polygonal overgrowth of brucite.

To determine mineral saturation indices at temperature, the experimental pH must be calculated. Log K values for the major element speciation and mineral precipitation reactions were sourced from SUPCRT92 (Johnson *et al.* 1991). An Excel spreadsheet linked to EqSolvR was constructed (Mroczek S. and Mroczek E., 2017) to do an iterative computation to determine the seawater speciation at temperature. This calculates the free activity of Mg^{2+} and Ca^{2+} in solution and the correct pH for 400°C, 500 bar. Using an average pH of 3.0 for the seawater portion of the experiment, the pH is calculated to be 5.25 and log Q of the brucite (a) and anhydrite (d) precipitation reactions are +6.9 and -4.322, respectively. This gives mineral saturations indices for brucite and anhydrite as +0.038 and +0.0053. The shows that the heated seawater was saturated with respect to these minerals. This calculation cannot be done for epsomite and MHSH(Mg1.5) as thermodynamic data do not exist for these phases at 400°C.

As seawater contains very little silica (<0.1 mg kg^{-1}) and iron (<0.1 mg kg^{-1}), the SiO_2 and Fe present in the effluent must be released from the zirconia beads. It is noted that an increase in the mobility of iron occurred after the switch to seawater. This is due to higher solubility as a result of the formation of Fe chloride complexes and the low pH.

5. CONCLUSION

The experiments have permitted measurement of the equilibria active in heated seawater at near-supercritical conditions (400°C, 500 bar). These conditions are achieved within the oceanic crust in submarine hydrothermal systems at depth (4-5 km). As seawater descends into the recharge zone of mid-ocean ridges, it is progressively heated. In the experiment, this process has been partially simulated. While the experiment did not replicate the natural environment exactly, i.e., there was no fluid-rock interaction during heating. It did reproduce the process of retrograde mineral precipitation leading to acidification of the fluid. The experimental apparatus thus allows us to simulate the process of seawater-rock interaction in a flowing environment.

Preliminary results show the following:

- seawater is depleted in calcium, magnesium and sulfate due to the precipitation of retrograde solubility sulfate phases and brucite;
- the precipitation of these minerals occurs rapidly achieving saturation in a short period of time (hours?);
- experimental pH has been successfully calculated using existing thermodynamic data verifying equilibrium in the experiments;
- the acidic pH values confirm the role of Mg and Ca in lowering seawater pH in the recharge zone;
- it is predicted that the introduction of such low pH seawater into rock material at near-supercritical condition will have extensive effects on the resulting fluid-rock interactions.

The experiment using seawater and basalt is currently underway to investigate this process.

AKNOWLEDGEMENTS

The authors wish to acknowledge support from the Government of New Zealand through funding of the GNS Geothermal Resources of New Zealand research programme.

REFERENCES

Johnson J.W., Oelkers, E.H., and Helgeson, H.C., 1991, SUPCRT92:A software package for calculating the standard molal thermodynamic properties of minerals, gases, aqueous species, and reactions from 1 to 5000 bars and 0˚ to 1000˚C: Computers and Geosciences (submitted).

Mroczek S., Mroczek E. (2017). EqSolvR: Chemical Equilibrium Solver. R package version 1.1.0. (https://github.com/shearwavesplitter/EqSolvR.

Passarella M., Mountain B.W., Seward., T.M., (2017). Experimental Simulations of Basalt-fluid Interaction at Supercritical Hydrothermal Condition (400°C – 500bar). *Procedia Earth and Planetary Science*. Vol. 17, pp 770-773.

Passarella M., Mountain W., B., Zarrouk, S., & Burnell, J., (2015). Experimental simulation or re-injection of non-condensable gases into geothermal reservoirs: greywacke-fluid rock interaction. Proceeding, *37th New Zealand Geothermal Workshop, 2015*.

Seyfried W. E., Berndt, M.E., and Seewald, J.S., (1988). Hydrothermal alteration processes at mid-ocean ridges: Constraints from diabase alteration experiments, hot-spring fluids and composition of the oceanic crust. *Canadian Mineralogist*. Vol. 26, pp 787-804.

Sonney R., Mountain B.W., (2013). Experimental simulation of greywacke—fluid under geothermal conditions. *Geothermics* vol. 47, pp. 27-39.